Biogeosciences Discuss., 12, 15925–15945, 2015
www.biogeosciences-discuss.net/12/15925/2015/
doi:10.5194/bgd-12-15925-2015

Biogeosciences
Discussions
Open Access

Comparing solubility algorithms of greenhouse gases in Earth-System modelling

V. M. N. C. S. Vieira[1], **E. Sahlée**[2], **P. Jurus**[3,6], **E. Clementi**[4], **H. Pettersson**[5], **and M. Mateus**[1]

[1]MARETEC, Instituto Superior Técnico, Universidade Técnica de Lisboa, Av. Rovisco Pais, 1049-001, Lisboa, Portugal
[2]Dept. of Earth Sciences, Air Water and Landscape sciences, Villavägen 16, 75236 Uppsala, Sweden
[3]DataCastor, Prague, Czech Republic
[4]Istituto Nazionale di Geofisica e Vulcanologia, INGV, Bologna, Italy
[5]Finnish Meteorological Institute, P.O. Box 503, 00101 Helsinki, Finland
[6]Institute of Computer Science, Czech Academy of Sciences, Czech Republic

Received: 2 September 2015 – Accepted: 3 September 2015 – Published: 28 September 2015

Correspondence to: V. M. N. C. S. Vieira (vasco.vieira@tecnico.ulisboa.pt)

Published by Copernicus Publications on behalf of the European Geosciences Union.

Abstract

Accurate solubility estimates are fundamental for (i) Earth-System models forecasting the climate change taking into consideration the atmosphere–ocean balances and trades of greenhouse gases, and (ii) using field data to calibrate and validate the algorithms simulating those trades. We found important differences between the formulation generally accepted and a recently proposed alternative relying on a different chemistry background. First, we tested with field data from the Baltic Sea, which also enabled finding differences between using water temperatures measured at 0.5 or 4 m depths. Then, we used data simulated by atmospheric (Meteodata application of WRF) and oceanographic (WW3-NEMO) models of the European Coastal Ocean and Mediterranean to compare the use of the two solubility algorithms in Earth-System modelling. The mismatches between both formulations lead to a difference of millions of tons of CO_2, and hundreds of tons of CH_4 and N_2O, dissolved in the first meter below the sea surface of the whole modelled region.

1 Introduction

Atmosphere–ocean gas exchange is a relevant contemporary subject due to the role of the oceans in the global biogeochemical cycles and their potential as sinks for greenhouse gases, thus eventually acting as climate change mitigators. In the pole regions, the solubility pump retrieves large amounts of greenhouse gases from the atmosphere and transports them to the deep ocean. On the other hand, the coastal ocean and upwelling zones are traditionally considered as spots of CO_2 outgassing. These fluxes of gases across the air–water interface are given by $F = k_{\mathrm{w}}\,(C_{\mathrm{a}}/k_{\mathrm{H}} - C_{\mathrm{w}})$, in units of mol m^{-2} s^{-1}. C_{a} and C_{w} are the air and water gas concentrations in mol m^{-3}, k_{H} is Henry's constant for the gas specific solubility, here in its scalar ($C_{\mathrm{a}}/C_{\mathrm{w}}$) form, and k_{w} the gas transfer velocity across the air–water infinitesimally thin surface layer, in m s^{-1} although usually plotted in cm h^{-1}. An alternative formulation estimates $F = k_{\mathrm{w}} \cdot k_{\mathrm{H}} cp$

$\cdot \Delta p_{\text{gas}}$, with Δp_{gas} being the difference between air and water gas partial pressures (atm) and $k_{\text{H}}cp$ the Henry's constant in its equivalent $C_{\text{w}}/p_{\text{a}}$ form ($\text{mol}\,\text{m}^{-3}\,\text{atm}^{-1}$). Frequently, the difference between air and water gas concentrations measured in parts-per-million (Δ ppm) is used as a proxy for Δp_{gas}. From these formulations can be seen that, similarly to electric currents or water streams, air–water gas fluxes have two components: (i) a potential difference (unbalance) between two compartments, in this case air and water concentrations, setting a strength and direction of a flux. To this matter, the world oceans, and particularly the coastal oceans, are very heterogenic in their greenhouse gas unbalance with the atmosphere, and with a fine resolution and intricacy of processes, associated to upwelling, plankton productivity and continental loads. This holds for CO_2 (Smith and Hollibaugh, 1993; Cole and Caraco, 2001; Takahashi et al., 2002, 2009; Inoue et al., 2003; Duarte and Prairie, 2005; Borges et al., 2005; Rutgersson et al., 2008; Lohrenz et al., 2010; Torres et al., 2011; Oliveira et al.; 2012; Rödenbeck et al., 2013; Schuster et al., 2013; Landschützer et al., 2014; Arruda et al., 2015; Brown et al., 2015) for CH_4 (Harley et al., 2015) and for N_2O (Bange et al., 1996; Nevison et al., 1995, 2004; Walter et al., 2006; Barnes and Goddard, 2011; Sarmiento and Gruber, 2013). But an unbalance can also occur within the open ocean at the fine resolution of mesoscale eddies depending on thermodynamic balance, primary productivity and the time the upwelled water has remained on the surface and departed its cold-core (Chen et al., 2007), or at the larger scale of the Weddell Gyre (Brown et al., 2015). The other component affecting the flux is (ii) the resistance the medium does to being crossed by a flow. The transfer velocity at which gases cross the infinitesimally thin air–water interface is highly dependent on turbulence upon it. This, in its turn is dependent on its forcings, namely wind drag, wave breaking, currents and rain, and its antagonizers, namely the sea-surface viscosity set by the water properties and presence of surfactants. With all these sources of variability, transfer velocity assumes a vital role as mediator of atmosphere–ocean gas exchanges and the development of its estimator algorithms becomes a fundamental aspect. The literature has tens of such algorithms relying in different theoretical backgrounds and either fitted to specific sea-surface conditions or rougher generalizations. In order to calibrate them, the transfer velocities can be estimated from field data reworking the flux equations as: $k_\mathrm{w} = F/(C_\mathrm{a}/k_\mathrm{H} - C_\mathrm{w})$ or $k_\mathrm{w} = F/(k_\mathrm{H} cp \cdot \Delta p_\mathrm{gas})$. The gas flux ($F$) is measured in the field with a variety of techniques. The floating dome measures the change in the gas concentration inside a container whose only open side faces the sea-surface (Frankignoulle, 1988). One of the first that used the eddy-covariance method to study the atmosphere–ocean gas fluxes was the COARE experiment (Fairall et al., 1996). Since then, the method has been applied in a growing number of studies (e.g. McGillis et al., 2001, 2004; Rutgersson et al., 2008; Ho et al., 2011). Because the difference in air–water concentrations sets a positive flux downward whereas eddy-covariance methods, being originated from micro-meteorology, traditionally set positive fluxes upward, there must be a rectification by $-F$ or $-k_\mathrm{w}$ in the formulas above (Woolf, 2005; Zhang et al., 2006). The dual-tracer method, vastly applied to wind tunnel experiments in the late 1970's–1980's, can only average a flux over a wide time interval (Watson et al., 1991).

Accurate k_H estimates are of utmost importance for Earth-System modelling: (i) they report atmosphere–ocean greenhouse gas equilibrium against which unbalances are estimated, (ii) in dual-layer models, they weight air-side and water-side sea-surface thin layers through which gasses must be transferred, and (iii) they are essential to calibrate air–water gas transfer velocity formulations. Starting in the 1970's, several authors developed solubility formulations for several gases including the greenhouse gases CO_2, CH_4 and N_2O. Sarmiento and Gruber (2013) compiled a general algorithm together with each gas' specific constants, to estimate solubility accounting for water temperature, salinity, non-ideal gas behaviour and moisture partial pressure. Recently, Johnson (2010) developed an alternative algorithm accounting for temperature, salinity, the molecular and thermodynamic properties of the water, its solutes and the specified gas, but disregarding the non-ideal behaviour of the gases and moisture. We compared the two formulations, as well as using the bulk or sea-surface water temperatures, by testing their solubility and transfer velocity estimates. All formulations were included in the Maretec model and software (http://www.maretec.org/en/publications/, <this publication>, <Download zip>) whose development started by Vieira et al. (2013, 2015).

2 Methods

The two formulations were tested with field data from the atmospheric tower at Östergarnsholm in the Baltic Sea (57°27′ N, 18°59′ E), a Submersible Autonomous Moored Instrument (SAMI-CO_2) 1 km away and a Directional Waverider (DWR) 3.5 km away, both south-eastward from the tower (e.g. Rutgersson et al., 2008 and Högström et al., 2008 for detailed description of the sites). The measurement period was from the 22 to the 26 May 2014. The air–water fluxes were measured by the eddy-covariance method, calculated over 30 min bins and corrected according to the Webb–Pearman–Leuning (WPL) method (Webb et al., 1980). Only the fluxes for which the wind direction set the SAMI-CO_2 and DWR in the footprint of the atmospheric tower ($90^\circ <$ wind direction $< 180^\circ$) were used. The SAMI-CO_2 measured temperature at a depth of 4 m, which we take as representative for the bulk water temperature. The DWR measured temperatures at a depth of 0.5 m, taken here as representative for a closer to sea-surface temperature. The solubility algorithms were tested for the effects of using either temperature measurements. Salinity was obtained from the Asko mooring data provided by the Baltic In Situ Near Real Time Observations available in the MyOcean catalogue. The competing formulations were also tested with simulated data relative to the European shores from the 24 May 2014 at 06:00 to the 27 May 2014 at 00:00 LT. The air temperature and pressure were retrieved from the lowest level Meteodata.cz standard operational application of the Weather Research and Forecasting Model (WRF) model with 9 km and 1 h resolutions. Over the ocean, the lowest level was never higher than a few centimetres. Sea-Surface Temperature (SST) and salinity (S) were estimated from the Nucleus for European Modelling of the Ocean (NEMO) numerical framework provided in MyOcean catalogue using 1 m thick vertical layers (from the surface down to 20 m depth), 1/12° horizontal and 1 day resolutions. All variables were interpolated to the same 0.09° horizontal grid (roughly 11 km at Europe's latitude) and 1 h time steps.

2.1 Sarmiento and Gruber (2013) compilation – "Sar13"

The algorithm for temperature and salinity dependence of k_{Hcp} provided by Weiss (1974) and Weiss and Price (1980) has been extensively adapted and applied to other gases. We converted its compilation by Sarmiento and Gruber (2013) to its scalar k_H form preserving the a_i and b_i constants (from their Table 3.2.2) required to estimate Bunsen's solubility coefficient β. This formulation accounted for fugacity (f) of non-ideal gases (Eq. 1) and corrected the gas partial pressure for moisture effects ($p_{moist} = (1 - p_{H_2O}/P)p_{dry}$) considering water vapour saturation over the sea-surface (Eq. 2). P is air pressure (atm), T_w is water temperature (K), S is salinity (‰), p is partial pressure (atm), R is the ideal gas law constant ($\mathrm{Pa\,m^3\,mol^{-1}\,K^{-1}}$), V_m is the molar volume of the specific gas (22.3 for CO_2 and CH_4, and 22.2432 for N_2O) and $V_{ideal} = 22.4136\,\mathrm{mol\,L^{-1}}$ is the molar volume of ideal gases. Solubility coefficients were estimated from the Virial expansion (Eq. 3), where B was β or β/V_m, depending on which gas it was applied to (see Table 3.2.2 from Sarmiento and Gruber, 2013). The software automatically detected it from the a_i coefficient. When $B = \beta$ the k_H was estimated from Eq. (4). When $B = \beta/V_m$ the k_H was estimated from Eq. (5).

$$f = \exp\left(\frac{101.325P\left(V_m - V_{ideal}\right)}{RT_w}\right) \tag{1}$$

$$\frac{p_{H_2O}}{P} = \exp\left(24.4543 - 67.4509\left(\frac{100}{T_w}\right) - 4.8489\ln\left(\frac{T_w}{100}\right) - 0.000544S\right) \tag{2}$$

$$\ln(B) = a_1 + a_2\frac{100}{T_w} + a_3\log\frac{T_w}{100} + a_4\left(\frac{T_w}{100}\right)^2 + S\cdot\left(b_1 + b_2\frac{T_w}{100} + b_3\left(\frac{T_w}{100}\right)^2\right) \tag{3}$$

$$k_H = \left(1 - \frac{p_{H_2O}}{P}\right)\frac{101.325V_m}{RT_w\beta f} \tag{4}$$

$$k_{\mathrm{H}} = \frac{101.325}{RT_{\mathrm{w}}\beta f} \tag{5}$$

2.2 Johnson (2010) formulation – “Joh10”

An extensive list of Henry’s constants in their $C_{\mathrm{w}}/p_{\mathrm{a}}$ form was made available by Sander (1999). These report the solubilities of many gases at 25 °C (298.15 K) and 0 ‰. We used its inverse $k_{\mathrm{H}}pc$ (the $p_{\mathrm{a}}/C_{\mathrm{w}}$ form), which for CO_2 is 29.4, for CH_4 is 714.3 and for N_2O is 40 L atm mol^{-1}. Equation (6) converted $k_{\mathrm{H}}pc$ to k_{H} at a given temperature and 0 ‰ salinity. The term $-\Delta_{\mathrm{soln}}H/R$ reflected the temperature (in Kelvin) dependence of solubility (see Sander, 1999), having a value of 2400 for CO_2, 1700 for CH_4 and 2600 for N_2O. The correction to a given salinity required a provisional $k_{\mathrm{H\#}} = 0.0409 \cdot k_{\mathrm{H}}pc$ to estimate θ from Eq. (7). The liquid molar volume of the gas at its boiling point (Vb) was estimated using the additive Schroeder method. Vb and θ were required to estimate the empirical Setschenow constant $\mathrm{Ks} = \theta \cdot \log \mathrm{Vb}$. Finally, $k_{\mathrm{H,0‰}}$ was corrected for salinity as $k_{\mathrm{H}} = k_{\mathrm{H,0‰}} \cdot 10^{\mathrm{Ks}\cdot S}$.

$$k_{\mathrm{H,0‰}} = \frac{12.1866 \cdot k_{\mathrm{H,pc}}}{P \cdot T_{\mathrm{w}} \cdot e^{-\frac{\Delta_{\mathrm{Soln}}H}{R}\left(1/T_{\mathrm{w}} - 1/298.15\right)}} \tag{6}$$

$$\theta = 7.33532 \times 10^{-4} + 3.39615 \times 10^{-5} \cdot \log(k_{\mathrm{H\#}}) - 2.40888 \times 10^{-6} \cdot \log(k_{\mathrm{H\#}})^2 + 1.57114 \times 10^{-7} \cdot \log(k_{\mathrm{H\#}})^3 \tag{7}$$

3 Results

The wind direction set the SAMI-CO_2 and the DWR in the footprint of the atmospheric tower only for the first 1.5 days of the experiment, during which the atmospheric pressure and the water temperature vertical profile at the two depths varied (Fig. 1), while salinity was rather constant around 6.34 ± 0.02 ppt. The solubilities estimated using the algorithms by Johnson (2010) and by Sarmiento and Gruber (2013) fairly matched. Nevertheless, their divergence increased the more the solubility departed from 1 (Fig. 1). This resulted either from: (i) the insoluble nature of the gas, in the case of CH_4, or (ii) the changes in water temperature, in the cases of CO_2 and N_2O. Overall, their roughly 1 % solubility differences when applied to the fairly soluble CO_2 increased to roughly 3.2 % when applied to the rather insoluble CH_4. Far worst mismatches occurred between solubilities estimated using water temperatures at the two different depths (Fig. 1), which could go up to 6 % different in the CO_2 case.

A more thorough perspective of how much both formulations diverge was obtained testing T_w from 4 to 30 °C at 1 °C intervals and S from 0 to 36 ppt at 1 ppt intervals, while preserving the remaining environmental conditions as observed during the t instances the wind blew from the footprint of the atmospheric tower. The formulations were compared by $k_{H,Joh10}/k_{H,Sar13}$, which being a ratio, was averaged over t using the geometric mean (Fig. 2). In the cases of CO_2 and N_2O, the two formulations diverge further with saline cooler waters, as occur in the polar regions, and with less-saline warmer waters, as occur in the coastal ocean adjacent to big river estuaries, such as the Amazon, Orinoco, Mississipi, Missouri or Nile. In the case of CH_4, the two formulations diverge more at both temperature extremes.

From the 24 to the 26 May, the water temperature at the first meter below the European coastal ocean surface changed significantly and there was a significant fresh water input from the Black Sea and the Baltic Sea (Video 1). The widest divergences in CO_2 solubility estimates were up to 4.5 % of the solubility and associated to cooler waters, the widest divergences in the CH_4 solubility estimates were up to 5.8 % of the solubility and associated to both temperature extremes, and the widest divergences in the N_2O solubility estimates were up to 2.1 % of the solubility and associated to cooler and less saline waters (Fig. 2). These mismatches between forecasted solubilities had an impact on the mass balances of the modelled biogeochemical cycles leading to wide differences in the quantities of greenhouse gas dissolved in the first meter below the ocean surface (Fig. 3). This difference was estimated as

$\Delta \mathrm{t\,m}^{-1}\, 121\,\mathrm{km}^{-2} = 11^2 \cdot \Delta s \cdot p_{\mathrm{gas}} \cdot P \cdot 101\,325 \cdot M_{\mathrm{a}} / (10^9 \cdot R \cdot T)$, where Δs was the difference in the solubility estimated by either algorithm in its $C_{\mathrm{w}}/C_{\mathrm{a}}$ form at each 11 km wide cells and averaged over the 66 h time interval, $M_{\mathrm{a}} = 28.97$ was the air molecular mass and p_{gas} was the atmospheric partial pressure of CO_2, CH_4 or N_2O, respectively 390, 1.75 and 0.325 ppm (EPA, 2015) under the assumption they were approximately uniform all over the atmospheric surface boundary layer. The differences alone summed to 3.86×10^6 t of CO_2, 880.7 t of CH_4 and 401 t of N_2O. Because the bias of N_2O changed from positive to negative with location, the resulting bias integrated over the whole area was 163 t.

The transfer velocities estimated from the eddy-covariance data showed only small differences. The worst mismatch was a difference (Δk_{600}) of 0.3 cm h^{-1} when the transfer velocity (k_{600}) was 36 cm h^{-1}. The measurements were from the Baltic Sea where the low surface salinity and temperature did not promote much of a difference between the k_{H} estimated by either formulation, and hence did not propagate a mismatch to the k_{600} estimates. However, simulating a situation with open ocean salinities (35 ppm), the difference Δk_{600} between the two algorithms was around 4.5 % of the k_{600} (Fig. 4). This difference should increase with lower water temperatures. The effect of water temperatures measured from different depths was not perceptible.

4 Discussion

Both formulations diverge considerably in their form and background. The Weiss (1974) and Weiss and Price (1980) algorithm, compiled by Sarmiento and Gruber (2013), used the popular Virial equation for an estimation of the effects of temperature and salinity on the Bunsen solubility coefficients. Therefore, their process-oriented description of solubility relies on the ideal gas law. Then, fugacity is estimated to correct for non-ideal gas behaviour, important for gases like CO_2, CH_4 and N_2O (Weisenburg and Guinasso, 1979; Weis and Price, 1980; Sarmiento and Gruber, 2013), and moisture effects correct the gas atmospheric partial pressure. The formulation by Johnson (2010), an upgrade from Sander (1999), bases its process-oriented description of solubility on the molecular structure and thermodynamic properties of the gases. It is remarkable how both algorithms can converge to rather similar results despite their mathematical dissimilarities. However, the more uneven are the atmosphere and ocean gas partial pressures at steady state the more divergent are the solubilities estimated by both formulations. This happens either because the gas is rather insoluble or because the ocean surface temperature and/or salinity promote that unbalance. This mismatch points out that at least one of the algorithms systematically fails its forecasts, and it can well be both, although this work could not determine which one is it. Nevertheless, within the spatial and time frame of the experiment, this error could lead to a bias of 0.045 mol of CO_2 in the ocean surface per mol of CO_2 in the atmosphere, 0.0015 $\mathrm{mol\,mol^{-1}}$ of CH_4 and 0.012 $\mathrm{mol\,mol^{-1}}$ of N_2O. Furthermore, these biases occur in the most sensitive situations for Earth-System modelling: the cooler waters occur closer to the poles, where the solubility pump traps greenhouse gases and carries them to the deep ocean (Sarmiento and Gruber, 2013); both the warmer waters and the less saline waters occur in the coastal ocean and seas, and there is strong evidence the N_2O dissolved in the coastal ocean is unbalanced with the N_2O in the atmosphere (Bange et al., 1996; Nevison et al., 1995, 2004; Walter et al., 2006; Barnes and Goddard, 2011; Sarmiento and Gruber, 2013). Therefore, the biases of 3.86×10^6 t of CO_2, 880.7 t of CH_4 and 163 t of N_2O, estimated for the first meter depth of the European coastal ocean during late May 2014, may be an indicator of much higher global biases with stronger consequences. It would not be surprising that former simulations of greenhouse gas exchange between the atmosphere and the world oceans (Nevison et al., 1995, 2004; Walter et al., 2006; Lohrenz et al., 2010; Barnes and Goddard, 2011; Torres et al., 2011; Vichi et al., 2011; Mattia et al., 2012; Oliveira et al., 2012; Rödenbeck et al., 2013; Schuster et al., 2013; Landschützer et al., 2014; Arruda et al., 2015) would arrive at quantitatively very different results if an alternative formulation was used. Presently, this 66 h averaged bias in the estimates of N_2O dissolved in the European coastal ocean represents about 2.4 % of the N_2O yearly discharged by European estuaries, as estimated by Barnes and Goddard (2011). Significant bias in the estimation of the marine N_2O dynamics has already been reported (Nevinson et al., 2004; Denman et al., 2007; Jiang et al., 2007; Barnes and Goddard, 2011). Since marine systems contribute with 10 to 33 % of the tropospheric N_2O (Denman et al., 2007; Jiang et al., 2007), solving these potential sources of error is fundamental for a reliable Earth-System model forecasting the climate change. In Parallel, the current coarse resolution Earth-System models, by representing the Earth with approximately 1100 km wide cells, cannot possibly describe with accuracy the solubility heterogeneity that this work demonstrated to occur at the coastal ocean with a fine resolution and high impact in the mass balances of greenhouse gases.

Using the water temperature measured by the DWR at 0.5 m or by the SAMI-CO_2 at 4 m depths had a greater impact on the solubility estimates. Unfortunately, it is unknown how much of the temperature differences were due to the different depths or locations. Nevertheless, it is well known the SST steep vertical gradient originating from the warm-layer and cool-skin effects (Fairall et al., 1996; Zeng and Beljaars, 2005; Brunke et al., 2008). This work proved that a biased SST estimate may propagate to estimates of atmosphere–ocean greenhouse gas trades and balances, and thus the appropriate choices must be made. In order to estimate the atmosphere–ocean unbalanced gas partial pressures, the “warm layer” reporting the average temperature in the first few meters of water seems the obvious choice. However, when weighting the air-side and water-side thin surface layer, the “cool skin” water temperature should be used instead (Fairall et al., 1996; Zeng and Beljaars, 2005; Brunke et al., 2008). The many algorithms estimating the transfer velocity from the sea-surface state and the atmospheric surface boundary layer yield widely divergent results. Many factors contribute to it, like many of them having been calibrated under widely different ranges of environmental conditions. It has now been demonstrated that biased model calibrations based on biased estimates of solubility can also contribute to this error.

5 Conclusions

For long the Geosciences and Earth-System modelling have accepted the Weiss (1974) and Weiss and Price (1980) formulation as the reliable estimator of solubility. However, its discrepancies with a recent alternative formulation by Johnson (2010) suggest this may not be true. Therefore, both formulations need be extensively tested and validated in order to increase accuracy and confidence in the estimates of atmosphere–ocean greenhouse gas exchanges and in the results from Earth-System Models.

The Supplement related to this article is available online at doi:10.5194/bgd-12-15925-2015-supplement.

Author contributions. Software is available at http://www.maretec.org/en/publications/, V. Vieira developed the model and software, analysed the data and wrote the article; E. Sahlée provided the E-C and SAMI data; H. Pettersson provided the Directional Waverider data; P. Jurus provided the WRF data; E. Clementi provided the WW3 data; M. Mateus participated in the model and software development; all co-authors participated in the data analysis and reviewed the article.

References

Arruda, R., Calil, P. H. R., Bianchi, A. A., Doney, S. C., Gruber, N., Lima, I., and Turi, G.: Air–sea CO_2 fluxes and the controls on ocean surface pCO_2 variability in coastal and open-ocean southwestern Atlantic Ocean: a modeling study, Biogeosciences Discuss., 12, 7369–7409, doi:10.5194/bgd-12-7369-2015, 2015.

Bange, H. W., Rapsomanikis, S., and Andreae, M. O.: Nitrous oxide in coastal waters, Global Biogeochem. Cy., 10, 197–207, doi:10.1029/95GB03834, 1996.

Barnes, J. and Upstill-Goddard, R. C.: N_2O seasonal distributions and air–sea exchange in UK estuaries: implications for the tropospheric N_2O source from European coastal waters, J. Geophys. Res., 116, G01006, doi:10.1029/2009JG001156, 2011.

Borges, A. V., Delille, B., and Frankignoulle, M.: Budgeting sinks and sources of CO_2 in the coastal ocean: diversity of ecosystems counts, Geophys. Res. Lett., 32, L14601, doi:10.1029/2005GL023053, 2005.

Brown, P. J., Jullion, L. Landschützer, P., Bakker, D. C. E, Garabato, A. C. N., Meredith, M. P., Torres-Valdés, S., Watson, A. J., Hoppema, M., Loose, B., Jones, E. M., Telszewski, M, Jones, S. D., and Wanninkhof, R.: Carbon dynamics of the Weddell Gyre, Southern Ocean, Global Biogeochem. Cy., 29, 288–306, 2015.

Brunke, M. A., Zeng, X., Misra, V., and Beljaars, A.: Integration of a prognostic sea surface skin temperature scheme into weather and climate models, J. Geophys. Res., 113, D21117, doi:10.1029/2008JD010607, 2008.

Chen, F., Cai, W.-J., Benitez-Nelson, C., and Wang, Y.: Sea surface $p\mathrm{CO}_2$-SST relationships across a cold-core cyclonic eddy: implications for understanding regional variability and air–sea gas exchange, Geophys. Res. Lett., 34, L10603, doi:10.1029/2006GL028058, 2007.

Cole, J. J. and Caraco, N. F.: Carbon in catchments: connecting terrestrial carbon losses with aquatic metabolism, Mar. Freshwater Res., 52, 101–110, 2001.

Denman, K. L., Brasseur, G., Chidthaisong, A., Ciais, P., Dickinson, R. E., Hauglustaine, D., Heinze, C., Holland, E., Jacob, D., Lohmann, U., Ramachandran, S., da Silva Dias, P. L., Wofsy, S. C., and Zhang, X.: Couplings between changes in the climate system and biogeochemistry, in: Climate Change 2007: The Physical Science Basis. Contribution of Working Group I to the Fourth Assessment Report of the Intergovernmental Panel on Climate Change, edited by: Solomon, S., Qin, D. Manning, M., Chen, Z., Marquis, M., Averyt, K. B., Tignor, M., and Miller, H. L., Cambridge University Press, New York, 500–587, 2007.

EPA United States Environmental Protection Agency – Climate Change Indicators in the United States – Atmospheric concentrations of greenhouse gases, available at: http://www.epa.gov/climatechange/science/indicators/ghg/ghg-concentrations.html, last accessed: 27 August 2015.

Fairall, C. W., Bradley, E. F., Godfrey, J. S., Wick, G. A., Edson, J. B., and Young, G. S.: Cool-skin and warm-layer effects on sea surface temperature, J. Geophys. Res., 101, 1295–1308, 1996.

Frankignoulle, M.: Field measurements of air–sea CO_2 exchange, Limnol. Oceanogr., 33, 313–322, 1988.

Harley, J. F., Carvalho, L., Dudley, B., Heal, K. V., Rees, R. M., and Skiba, U.: Spatial and seasonal fluxes of the greenhouse gases N_2O, CO_2 and CH_4 in a UK macrotidal estuary, Estuar. Coast. Shelf S., 153, 62–73, 2015.

Ho, D. T., Sabine, C. L., Hebert, D., Ullman, D. S., Wanninkhof, R., Hamme, R. C., Strutton, P. G., Hales, B., Edson, J. B., and Hargreaves, B. R.: Southern Ocean Gas Exchange Experiment: setting the Stage, J. Geophys. Res., 116, C00F08, doi:10.1029/2010JC006852, 2011.

Högström, U., Sahlée, E., Drennan, W. M. Kahma, K. K., Smedman, A.-S., Johansson, C., Pettersson, H., Rutgersson, A., Tuomi, L., Zhang, F., and Johansson, M.: Boreal Environ. Res., 13, 475–502, 2008.

Inoue, H. Y., Ishii, M., Matsueda, H., Kawano, T., Murata, A., and Takasugi, Y.: Distribution of the partial pressure of CO_2 in surface water ($p\mathrm{CO}_2^{\mathrm{w}}$) between Japan and the Hawaiian Islands: $p\mathrm{CO}_2^{\mathrm{w}}$–SST relationship in the winter and summer, Tellus B, 55, 456–465, 2003.

Jiang, X., Ku, W., Shia, R.-L., Li, Q., Elkins, J. W., Prinn, R. G., and Yung, Y. L.: Seasonal cycle of N_2O: analysis of data, Global Biogeochem. Cy., 21, GB1006, doi:10.1029/2006GB002691, 2007.

Johnson, M. T.: A numerical scheme to calculate temperature and salinity dependent air–water transfer velocities for any gas, Ocean Sci., 6, 913–932, doi:10.5194/os-6-913-2010, 2010.

Landschützer, P., Gruber, N., Bakker, D. C. E., and Schuster, U.: Recent variability of the global ocean carbon sink, Global Biogeochem. Cy., 28, 927–949, 2014.

Lohrenz, S. E., Cai, W. J., Chen, F., Chen, X., and Tuel, M.: Seasonal variability in air–sea fluxes of CO_2 in a river-influenced coastal margin, J. Geophys. Res.-Oceans, 115, C10034, doi:10.1029/2009JC005608, 2010.

Mattia, G., Vichi, M., Zavatarelli, M., and Oddo, P.: The wind-driven response of the Mediterranean sea biogeochemistry to the Eastern Mediterranean Transient. A numerical model study, Geophys. Res. Abstr., 14, EGU2012-4437, 4437 pp., 2012.

McGillis, W. R., Edson, J. B., Ware, J. D., Dacey, J. W. H., Hare, J. E., Fairall, C. W., and Wanninkhof, R.: Carbon dioxide flux techniques performed during GasEx-98, Mar. Chem., 75, 267–280, 2001.

McGillis, W. R., Edson, J. B., Zappa, C. J., Ware, J. D., McKenna, S. P., Terray, E. A., Hare, J. E., Fairall, C. W., Drennan, W., Donelan, M., DeGrandpre, M. D., Wanninkhof, R., and Feely, R. A.: Air–sea CO_2 exchange in the equatorial Pacific, J. Geophys. Res., 109, C08S02, doi:10.1029/2003JC002256, 2004.

Nevison, C. D., Weiss, R. F., and Erickson III, D. J.: Global oceanic emissions of nitrous oxide, J. Geophys. Res, 100, 15809–15820, 1995.

Nevison, C. D., Lueker, T. J., and Weiss, R. F.: Quantifying the nitrous oxide source from coastal upwelling, Global Biogeochem. Cy., 18, GB1018, doi:10.1029/2003GB002110, 2004.

Oliveira, A. P., Cabeçadas, G., and Pilar-Fonseca, T.: Iberia coastal ocean in the CO_2 sink/source context: Portugal case study, J. Coastal Res., 28, 184–195, 2012.

Rödenbeck, C., Keeling, R. F., Bakker, D. C. E., Metzl, N., Olsen, A., Sabine, C., and Heimann, M.: Global surface-ocean $p\mathrm{CO}_2$ and sea–air CO_2 flux variability from an observation-driven ocean mixed-layer scheme, Ocean Sci., 9, 193–216, doi:10.5194/os-9-193-2013, 2013.

Rutgersson, A., Norman, M., Schneider, B., Petterson, H., and Sahlée, E.: The annual cycle of carbon dioxide and parameters influencing the air–sea carbon exchange in the Baltic Proper, J. Marine Syst., 74, 381–394, 2008.

Sarmiento, J. L. and Gruber, N.: Ocean Biogeochemical Dynamics, Princeton University Press, New Jersey, USA, 528 pp., 2013.

Sander, R.: Compilation of Henry's law constants for inorganic and organic species of potential importance in environmental chemistry (Version 3), 1999, available at: http://www.henrys-law.org (last access: 24 September 2015).

Schuster, U., McKinley, G. A., Bates, N., Chevallier, F., Doney, S. C., Fay, A. R., González-Dávila, M., Gruber, N., Jones, S., Krijnen, J., Landschützer, P., Lefèvre, N., Manizza, M., Mathis, J., Metzl, N., Olsen, A., Rios, A. F., Rödenbeck, C., Santana-Casiano, J. M., Takahashi, T., Wanninkhof, R., and Watson, A. J.: An assessment of the Atlantic and Arctic sea–air CO_2 fluxes, 1990–2009, Biogeosciences, 10, 607–627, doi:10.5194/bg-10-607-2013, 2013.

Smedman, A., Högström, U., Bergström, H., Rutgersson, A., Kahma, K. K., and Pettersson, H.: A case study of air–sea interaction during swell conditions, J. Geophys. Res.-Oceans, 104, 25833–25851, doi:10.1029/1999JC900213, 1999.

Smith, S. V. and Hollibaugh, J. T.: Coastal metabolism and the oceanic organic carbon balance, Rev. Geophys., 31, 75–89, 1993.

Takahashi, T., Sutherland, S. C., Sweeney, C. Poisson, A., Metzl, N., Tilbrook, B., Bates, N., Wanninkhof, R., Feelyf, R. A., Sabine, C., Olafsson, J., and Nojirih, Y.: Global sea–air CO_2 flux based on climatological surface ocean $p\mathrm{CO}_2$, and seasonal biological and temperature effects, Deep-Sea Res., 49, 1601–1622, 2002.

Takahashi, T., Sutherland, S. C., Wanninkhof, R., Sweeney, C., Feely, R. A., Chipman, D. W., Hales, B., Friederich, G., Chavez, F., Watson, A., Bakker, D. C. E., Schuster, U., Metzl, N., Yoshikawa-Inoue, H., Ishii, M., Midorikawa, T., Nojiri, Y., Sabine, C., Olafsson, J., Arnarson, Th. S., Tilbrook, B., Johannessen, T., Olsen, A., Bellerby, R., Körtzinger, A., Steinhoff, T., Hoppema, M., de Baar, H. J. W., Wong, C. S., Delille, B., and Bates, N. R.: Climatological mean and decadal changes in surface ocean $p\mathrm{CO_2}$, and net sea–air CO_2 flux over the global oceans, Deep-Sea Res. Pt. II, 56, 554–577, 2009.

Torres, R., Pantoja, S., Harada, N., González, H. E., Daneri, G., Frangopulos, M., Rutllant, J. A., Duarte, C. M., Rúiz-Halpern, S., Mayol, E., and Fukasawa, M.: Air–sea CO_2 fluxes along the coast of Chile: from CO_2 outgassing in central northern upwelling waters to CO_2 uptake in southern Patagonian fjords. J. Geophys. Res., 116, C09006, doi:10.1029/2010JC006344, 2011.

Vichi, M., Manzini, E., Fogli, P. G., Alessandri, A., Patara, L., Scoccimarro, E., Masina, S., and Navarra, A.: Global and regional ocean carbon uptake and climate change: sensitivity to an aggressive mitigation scenario, Clim. Dynam., 37, 1929–1947, 2011.

Vieira, V. M. N. C. S., Martins, F., Silva, J., and Santos, R.: Numerical tools to estimate the flux of a gas across the air–water interface and assess the heterogeneity of its forcing functions, Ocean Sci., 9, 355–375, 2013, http://www.ocean-sci.net/9/355/2013/.

Walter, S., Bange, H. W., Breitenbach, U., and Wallace, D. W. R.: Nitrous oxide in the North Atlantic Ocean, Biogeosciences, 3, 607–619, doi:10.5194/bg-3-607-2006, 2006.

Watson, A. J., Upstill-Goddard, R. C., and Liss, P. S.: Air–sea gas exchange in rough and stormy seas measured by a dual-tracer technique, Nature, 349, 145–147, 1991.

Webb, E. K., Pearman, G. I., and Leuning, R.: Correction of flux measurements for density effects due to heat and water vapour transfer, Quart. J. R. Meteorol. Soc., 106, 85–100, 1980.

Weisenburg, D. A. and Guinasso Jr., N. L.: Equilibrium solubilities of methane, carbon monoxide, and hydrogen in water and sea water, J. Chem. Eng. Data, 24, 356–360, 1979.

Weiss, R. F.: Carbon dioxide in water and seawater: the solubility of a non-ideal gas, Mar. Chem., 2, 203–215, 1974.

Weiss, R. F. and Price, B. A.: Nitrous oxide solubility in water and seawater, Mar. Chem., 8, 347–359,1980.

Woolf, D. K.: Parameterization of gas transfer velocities and sea state-dependent wave breaking, Tellus B, 57, 87–94, 2005.

Zeng, X. and Beljaars, A.: A prognostic scheme of sea surface skin temperature for modelling and data assimilation, Geophys. Res. Lett., 32, L14605, doi:10.1029/2005GL023030, 2005.

Zhang, W., Perrie, W., and Vagle, S.: Impacts of winter storms on air–sea gas exchange, Geophys. Res. Lett., 33, L14803, doi:10.1029/2005GL025257, 2006.

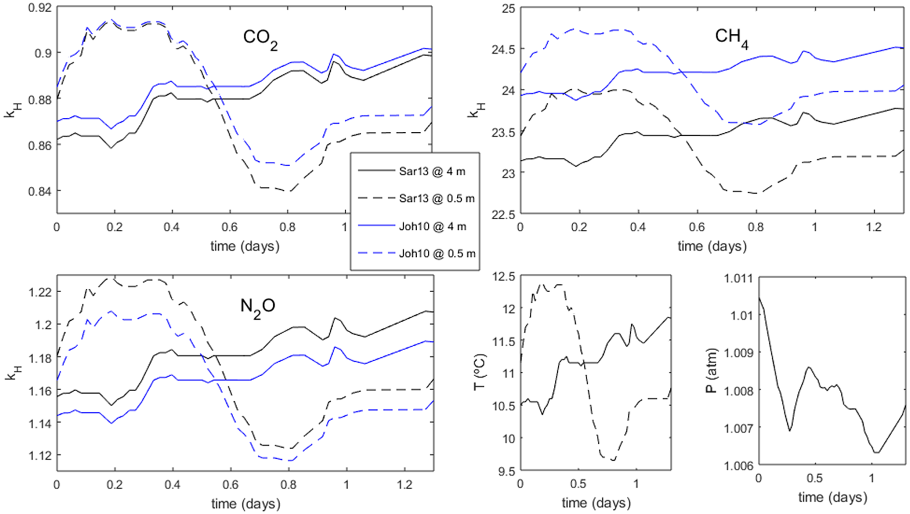

Figure 1. Solubility estimates for the Baltic Sea site: comparing algorithm by Johnson (2010) to compilation by Sarmiento (2013), and between using water temperature at 0.5 and 4 m depths.

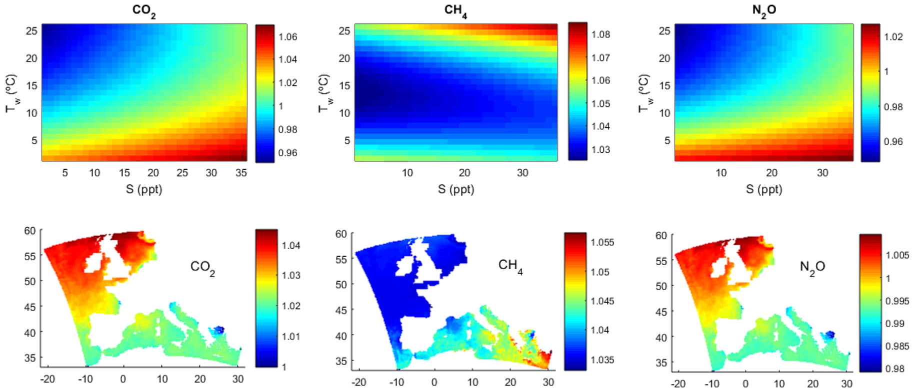

Figure 2. Comparison between solubility formulations: comparing solubility algorithm by Johnson (2010) to the compilation by Sarmiento and Gruber (2013). Colorscale: $k_{\mathrm{H“Joh10”}}/k_{\mathrm{H“Sar13”}}$.

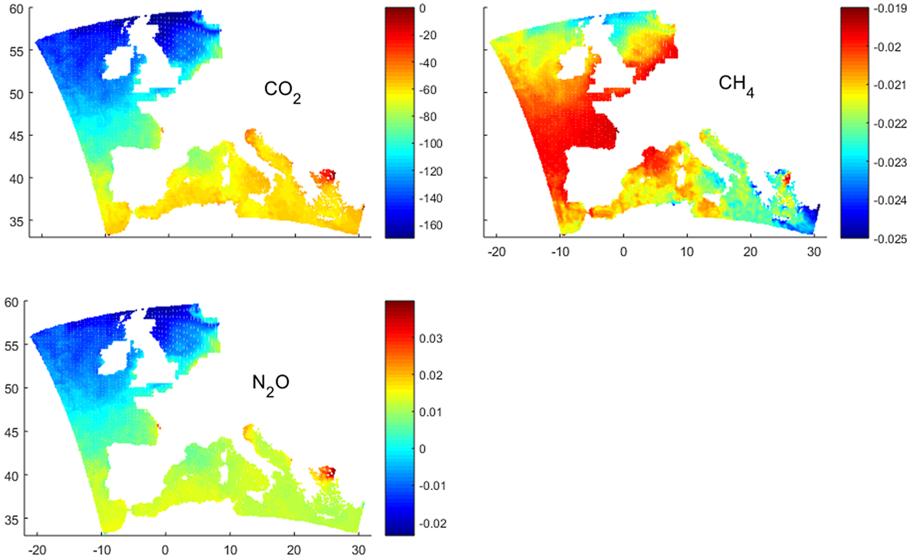

Figure 3. Bias in the gas mass balance for the European coastal ocean: comparing algorithm by Johnson (2010) to compilation by Sarmiento and Gruber (2013). Colorscale: $\Delta t\,m^{-1}\,121\,km^{-2}$ i.e, bias in the gas mass estimated by each algorithm (Δt) for the first meter depth (m^{-1}) in 11 km wide cells ($121\,km^{-2}$).

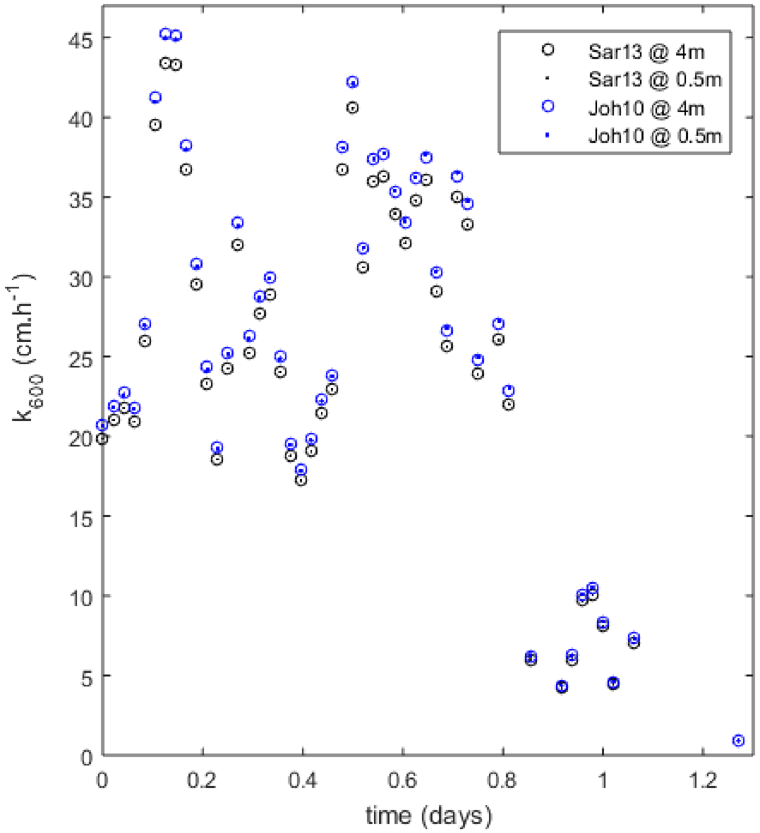

Figure 4. Bias in the observed transfer velocity of CO_2 across the atmosphere–ocean interface: comparison between using algorithm by Johnson (2010) or compilation by Sarmiento (2013), and between using water temperature at 0.5 and 4 m depths. Salinity was changed to 35 ‰.